

Diverse Signals Combinations for High-Sensitivity GNSS

Rigas T. Ioannides, L. Enrique Aguado,

(*University of Leeds*)

(Email: r.t.ioannides@leeds.ac.uk)

Gary Brodin

(*Pathtrack Ltd.*)

Indoor positioning imposes demanding requirements on the design of Global Navigation Satellite System (GNSS) sensors for both the acquisition and tracking functions. Although different combinations of coherent and non-coherent integration periods of a GNSS signal can be used to achieve reliable acquisition of the GNSS signals and indoors positioning, there are limitations to the extent that the integration period of the signal energy can be increased set by the receiver and satellite dynamics and the stability of the local oscillator. Assisting networks for GNSS applications (AGNSS) provide users with the capability of using long integration periods, enabling them to acquire indoor signals at low Carrier to Noise Ratio (CNR) values, where CNR is defined as the ratio of the received signal power over the noise density in units of dB-Hz. In this work we propose and evaluate the potential of a new method that will provide the user with an additional signal energy margin for accurate and reliable indoor positioning, with or without relying on assisted GNSS-type algorithms. The technique proposed here is based on the coherent and non-coherent combination of the energy of signals transmitted from the same GNSS satellite on different frequencies using the multiple open service signals that are to be provided by the Galileo system and under the GPS modernisation. This paper shows the improvement to the receiver acquisition and tracking performance using the proposed technique of combining energies at the L1, L2 and L5 bands for both data and pilot signals.

KEY WORDS

1. GNSS.
2. GNSS Signals.
3. Modernised GPS.
4. Galileo.

1. INTRODUCTION. Acquisition in indoor environments requires successful detection of signals at CNR values typically at the 14 dB-Hz level [1]. The acquisition complexity is commonly evaluated through the analysis of the probability of detection and false alarm of the algorithms employed. Long coherent integration periods have been used to enhance receiver signal sensitivity for indoor acquisition. Although such an approach increases the sensitivity of the receiver to frequency errors [2], user dynamics and oscillator stability [3], it can significantly improve the acquisition performance by increasing the CNR values at the correlation domain.

Algorithms have recently been proposed utilising the capabilities of the modernised GPS and Galileo signals to improve both acquisition and tracking. Those proposals focus on the combination of energy in the new signals in coherent and non-coherent manners, across the data and pilot signals at the same frequency [4,5]. Several strategies are used to increase the integration times in order to improve the acquisition performance in indoor environments, with different degrees of fully coherent and partial coherent processing [1]. A step further in this direction takes us to combine the energy across signals in different frequency carriers such that the combination would have a greater accumulated CNR with the consequent increased probability of detection. This work investigates the potential of this approach with different integration combinations to improve on the state of the art in terms of the probability of signal detection and thereafter the acquisition time at low CNR. More specifically, this work has been focused in combining the energies of the L1 and L5 signals, using both data and pilot signals for both GPS and Galileo systems. For GPS the L1 data signal is combined with the energy from the L5 data and pilot signals, using full coherent and partial coherent processing. In the Galileo case the data and pilot signals from the safety-of-life signals, L1 and E5b, have been processed using fully coherent and partial coherent processing, although the same ideas could apply for combining energy from the L2 carrier for the GPS case or E5a and/or E6 for Galileo.

In the remainder of this paper, the issues to be considered for combination of signals at different frequencies are identified and the effects both in terms of the overall acquisition search space and in terms of energy losses under worst case conditions are calculated. The benefits of the energy integration of the signals at L1 and L5 for GPS and Galileo systems are highlighted in terms of the decrease of the probability of false acquisition, or false alarm, compared to the case of using fully coherent and partial coherent processing of a single signal for the required value of probability of detection. The assessment of these benefits also includes the gain in acquisition time, according to a proposed verification algorithm.

2. BENEFITS FROM COHERENT AND PARTIAL COHERENT PROCESSING IN AN ASSISTED GNSS SYSTEM. Previous research [1,6] has investigated the benefits of using two different processing strategies in a high sensitivity AGNSS system, fully coherent processing and partial coherent processing. When using the fully coherent processing for a data channel, integration over the duration of a data bit requires knowledge of the sign of the data bit in order to avoid losses in the accumulation of the energy of the signal due to the possible transition of the data bit sign. On the other hand, if the data bit transition is known, partial coherent integration processing can accommodate long integration times by integrating over each data bit for both the I and Q arms of the signal, summing each coherently integrated period in a non-coherent manner. These two types of processing are shown in Figure 1.

Assisting data that is transmitted to the rover receiver by the means of a server or a base station and a communication channel can be used to increase the integration times. The assisting data usually includes satellite ephemeris and satellite clock error information, the navigation data stream, approximate location of the receiver, satellite signal transmission and differential corrections, mainly to estimate the

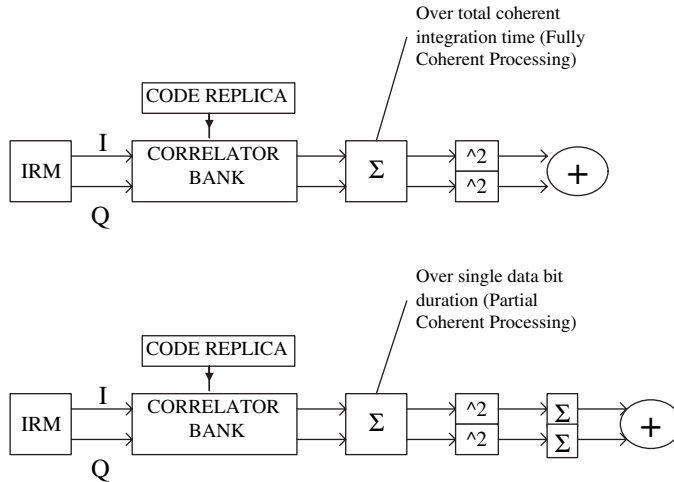


Figure 1. Fully and partial coherent processing.

ionospheric delays [7]. In the next sections, there is a discussion about the issues to be faced in the coherent integration of different frequency signals, together with the analysis of the simplifications that can be made in assisted GNSS applications.

3. COHERENT INTEGRATION OF DIFFERENT FREQUENCY SIGNALS. Several issues have to be considered when combining different signals from different frequencies that define the worst-case energy losses for the acquisition problem. This section presents an analysis of these issues.

3.1. *Different chip rates.* Depending on the accuracy of the satellite signal transmission time provided by the assisting server, the code search space can be restricted to a few hundreds of absolute code phases, or tens of microseconds, which can significantly reduce the search space. In the main framework of this paper, though, we assume that the transmission timing and the time transfer information that can be provided by the assisting network is not accurate enough to decrease the code search space; this is the case for most GSM networks.

In this case, as in the case of using a stand alone GNSS receiver, the code search space in the signal combination is determined by the longer code, the L5 code for GPS, while the correlator spacing is determined by the autocorrelation function (ACF) of the faster code, which is again the L5 code for GPS [8,9,10]. The same conclusions can also be made for the Galileo L1 (E1) and E5b signals, respectively [11]. A more detailed description of the signals is given in Table 1 for both GPS and Galileo.

For the modernised GPS constellation, the coherent combination of signals at different frequencies includes the combination of the L1 data signal with either the L5 data or pilot signals (I5 and Q5) but also the I5 with Q5 combination and the L1 with I5 and Q5 combination. The composite ACF of the L1+I5+Q5 combination is shown in Figure 2 assuming equal power for all three signals.

Although the code lengths for the L1-B/C and E5b signals for Galileo are different from those of GPS L1 and L5, the chip rates are the same. Additionally, the Galileo

Table 1. Present and future available GNSS signals.

SYSTEM	FREQUENCY (MHz)	CODE NAME	CHIP	CODE	Repetition	Repetition	DATA
			RATE Mchip/sec	LENGTH Chips	rate primary (ms)	rate (ms) Primary + secondary	
GPS	L1 (1575.42)	C/A	1.023	1023	1	1	50 bps
	L2 (1227.6)	L2C	1.023	10230	20	20	25 bps
	L5 (1176.45)	I5	10.23	10230X10	1	10	100 bps
	L5 (1176.45)	Q5	10.23	10230X20	1	20	Pilot
Galileo	L1 (1575.42)	L1B	1.023	4096	4	4	250 bps
	L1 (1575.42)	L1C	1.023	4096X25	4	100	Pilot
	E5a (1176.45)	E5a I	10.23	10230X20	1	20	50 bps
	E5a (1176.45)	E5a Q	10.23	10230X100	1	100	Pilot
	E5b (1207.14)	E5b I	10.23	10230X4	1	4	250 bps
	E5b (1207.14)	E5b Q	10.23	10230X100	1	100	Pilot

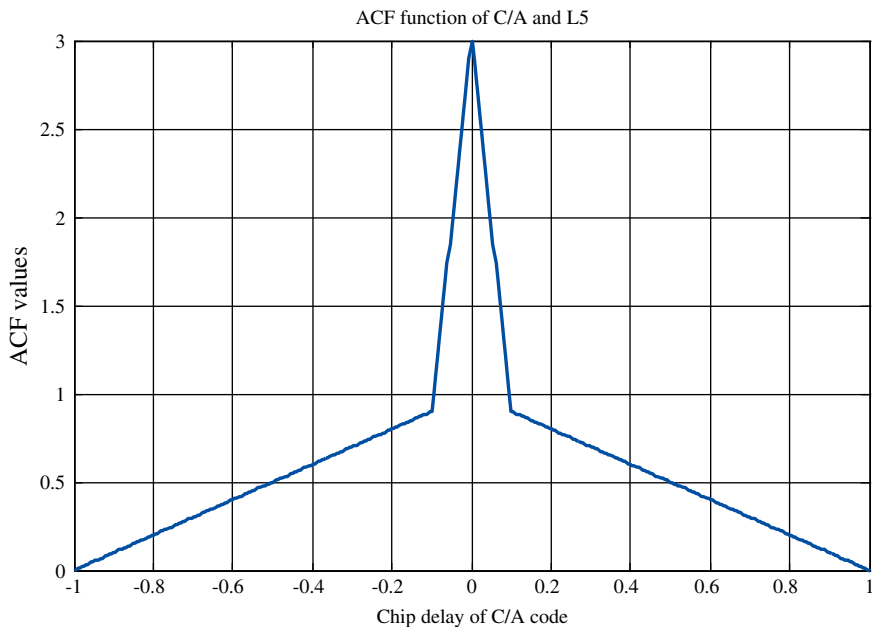


Figure 2. Composite ACF for L1 C/A+I5+Q5.

L1 signal will be BOC modulated. The ACF functions of the binary offset carrier (BOC) modulated signal, with a BOC (1,1) modulation, change depending on the acquisition method that is followed. This can be seen in Figure 3, where the absolute values of the ACF for the double sideband and the single sideband processing are shown. For Galileo the potential coherent combinations of signals are mainly the combination of the L1B with the L1C, or the E5b data with the E5b pilot, the coherent combination of the two pilot channels on L1 and E5b and the combination of all the four signals on L1 and E5b.

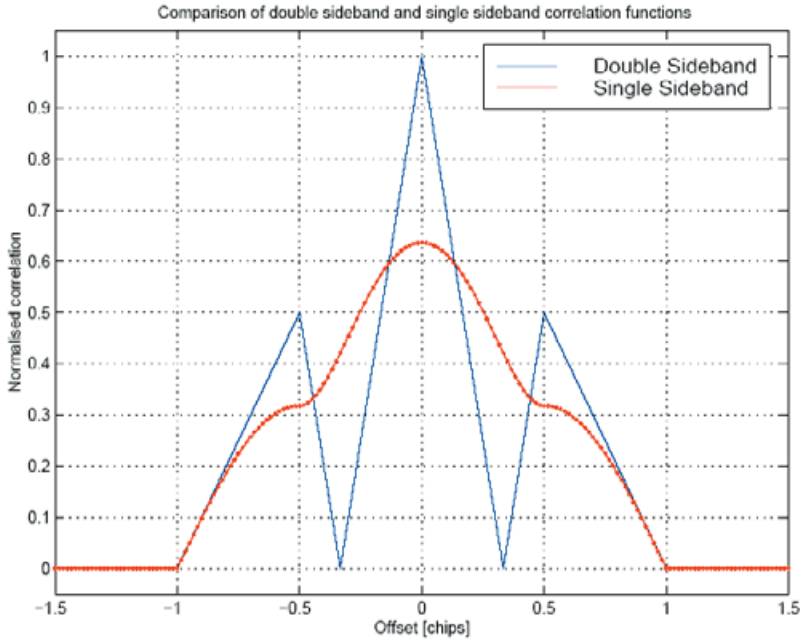


Figure 3. ACF functions for the BOC(1,1) L1 Galileo signal.

For a correlator spacing value $d_{L5} = 0.5$ L5 chips, the worst case expected correlation loss for the I5 and Q5 will be at 2.49 dB while for the L1 C/A code this spacing corresponds to 0.22 dB loss, as given using Equations 1 and 2 for L1 C/A and L5 respectively:

$$CSL_{d, L1} = 20 \cdot \log \left(1 - \frac{d_{L5}}{2} \cdot \frac{R_{C, L1}}{R_{C, L5}} \right) \tag{1}$$

$$CSL_{d, L1, Galileo} = 20 \cdot \log \left(1 - \frac{d_{L5}}{2} \cdot \frac{3R_{C, L1}}{R_{C, L5}} \right) \tag{1a}$$

$$CSL_{d, L5} = 20 \cdot \log \left(1 - \frac{d_{L5}}{2} \cdot \frac{R_{C, L5}}{R_{C, L5}} \right) \tag{2}$$

$$= 20 \cdot \log \left(1 - \frac{d_{L5}}{2} \right)$$

where CSL_d is the correlator spacing loss value for L1 and L5, d_{L5} is the correlator spacing in L5 chips and R_c denotes the chip rate for L1 C/A and L5 codes.

Depending on the type of the BOC signal processing there are different losses that will be associated with a $d_{L5} = 0.5$ of L5 (E5b) chips of correlator spacing. For DSB (Double Side-Band) since the slope of the BOC ACF function is 3 times steeper than the L1 C/A ACF the worst-case losses will be 0.67 dB for L1 using Equation 1a and 2.49 dB for E5b using Equation 2. If SSB (Single Side-Band) signal processing is chosen, the ACF function of the BOC signal can be assumed to be similar to that

of a BPSK signal, as in the GPS case, with an additional loss in signal energy close to 3.9 dB [13].

When using coherent integration times longer than the code's length, alignment to the NH (Neuman-Hoffman) code is required and this can be performed by using the minimum computational effort method presented in [12]. In the presence of assisting data both the navigation data bit and the NH code signs can be supplied to the user with minimum impact due to the delay in the communication link.

3.2. *Different frequency signals.* The following three issues have to be considered when combining signals at different frequencies:

3.2.1. *Different Doppler.* The Doppler of the L1 and L5 (E5b) signals will be different and so will their Doppler errors. In this work we initially investigated the performance of the coherent combination of different frequency signals seeking the least possible cost in terms of the search space. For this reason it is assumed that for each Doppler bin of L5 that is searched, the L1 carrier NCO can be scaled by F_{L1}/F_{L5} (or F_{L1}/F_{E5b} for Galileo) pointing to the L1 Doppler bin. This method will not increase the Doppler search space relative to the L5 Doppler search space. Considering this approach the Doppler search loss is calculated to be 0.9 dB for GPS L5 signals and 1.67 dB for the GPS L1 signal while for Galileo the Doppler search loss is calculated at 0.9 dB for E5b frequencies and 1.58 dB for L1 since the E5b frequency is slightly higher than the L5 frequency. These values were calculated based on a 1-msec coherent integration time and a Doppler bin search size of 500 Hz, using Equation 3:

$$\text{DOPPLER}_{\text{Loss}} = 20 \cdot \log_{10} (\sin(\pi \cdot \Delta f \cdot T_c) / (\pi \cdot \Delta f \cdot T_c)) \quad (3)$$

where Δf is the worst case Doppler search error assumed to be 250 Hz and T_c is the coherent integration time. Increasing the coherent integration time will also increase the number of Doppler bins and the resolution of the Doppler search space by the same factor, although the losses associated there will be the same.

3.2.2. *Relative code delays.* It is well known that the ionosphere is a dispersive medium, resulting in different code delays and phase advances for signals at different frequencies. The equation that gives the relative code delays due to the ionospheric propagation for L1 and L5 (or E5b in case of Galileo) signals is proportional to the inverse ratio of the squared frequencies of the two signals:

$$\text{RCD}_{\text{Ionosphere}} = 40.31 \cdot \text{TECU}_{\text{slant}} \cdot 10^{16} \cdot \left(\frac{1}{L5^2} - \frac{1}{L1^2} \right) \quad (4)$$

where L5, L1 are the frequencies of the signals in Hz and $\text{TECU}_{\text{slant}}$ is the slant TEC (Total Electron Content) value along the trans-ionospheric ray path of the signal, in TEC units [14]. *RCD* denotes the relative code delay in metres, which also implies that the ionospheric code delay for the lower frequency, L5 for GPS and E5b for Galileo, is always higher. Using previous research work, for a low elevation satellite at 10 degrees and for worst-case slant TEC values the maximum relative code delay for L1 and L5 or E5b frequencies was calculated to be at around 100 nanoseconds. The smaller ionospheric effect on the relative code delay will be when using a low TEC value and a satellite at zenith angle, which will account for almost 10 nanoseconds. If differential corrections are provided by the assisting data transmitted to the rover receiver, the relative code delay due to the ionosphere can be minimised.

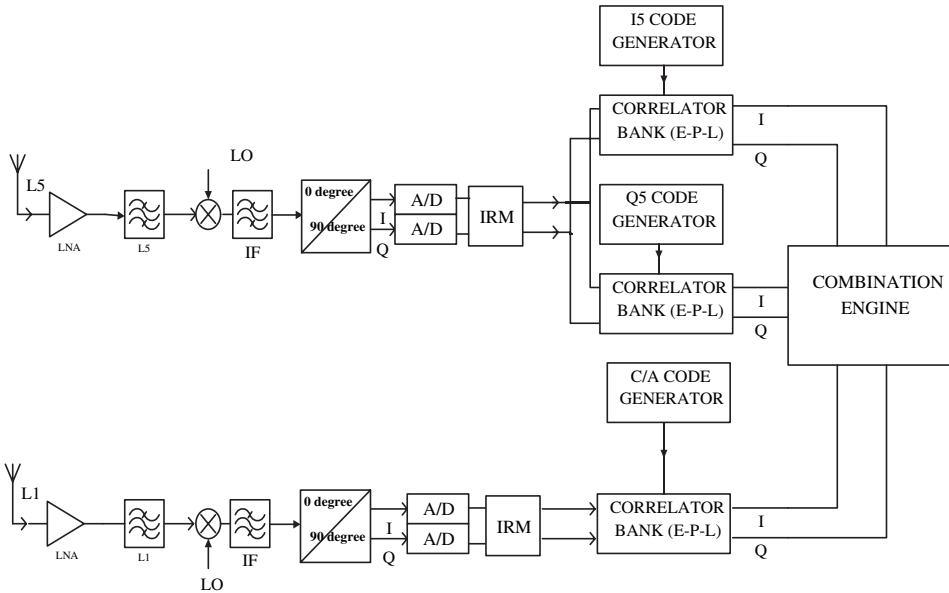


Figure 4. GPS L1 + L5 Architecture.

Filtering also introduces relative code delays, since the envelope of the signals are delayed through the filtering process. The relative delays that are introduced by the IF filtering, depend on the architecture chosen. For the architecture shown in Figure 4, where independent IF filters are used for the two frequencies, the group delay along the passband of the IF filters have been calculated using Butterworth filter theory [15] and shown in Figure 5, assuming 6th order Butterworth bandpass filters. GPS IF filter manufacturers [17] provide group delay variations across the passband of the filters, with the maximum group delay experienced at the edges of the passband of the filters, which is inline with the Butterworth filter type, and the mean group delay value being at the 150 nanoseconds level. Using Butterworth theory, for the wider bandwidth signal at L5, the group delay would be less than these values. Following this discussion the relative signal delay due to the IF filtering is not expected to exceed 100 nanoseconds for L1 and L5.

This worst case relative code delay value of 1 L5 chip has been considered for the evaluation of the benefits of the coherent combination of signals at different frequencies. For this work it has been assumed that the incoming codes are correlated with replica codes that are generated in a synchronous manner, as they are transmitted from the satellite. This would assess the benefits of the combination of the two signals, without increasing the search space to match the relative code delay of the two signals. For this situation the expected composite ACF for the Galileo case will be as shown in Figure 6, assuming that both signals are received with equal power. The losses that are associated with a $d_{L5} = 0.5$ of L5 chips correlator spacing and for 100 nanoseconds of relative group delay were found to be 0.7 dB for the L1 code while the L5 loss remains at the 2.49 dB. The same losses are considered in the case of the SSB processing of Galileo, while for the DSB processing method results in 2.2 dB of losses for L1, data and pilot, and 2.49 dB for L5. These expected

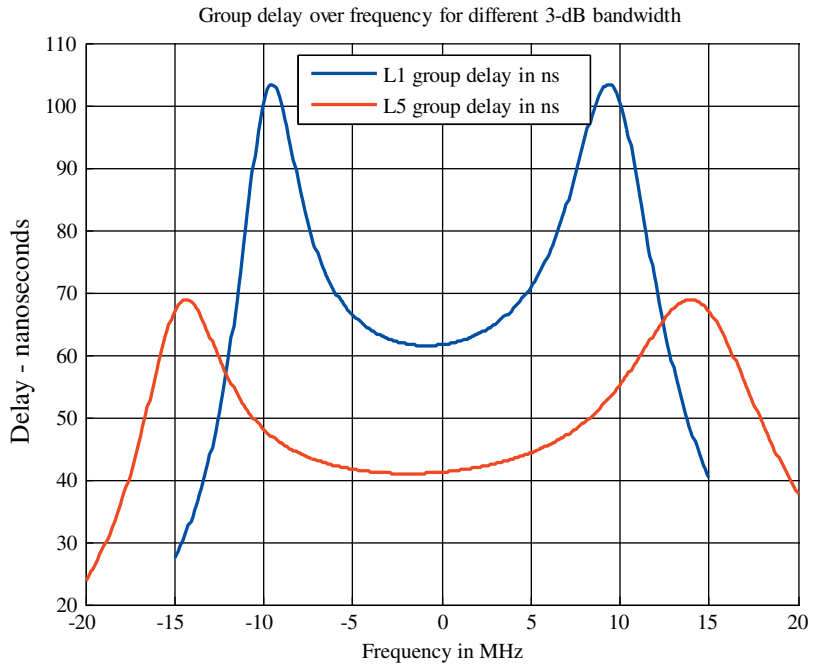


Figure 5. IF Butterworth type group delays for different bandwidths.

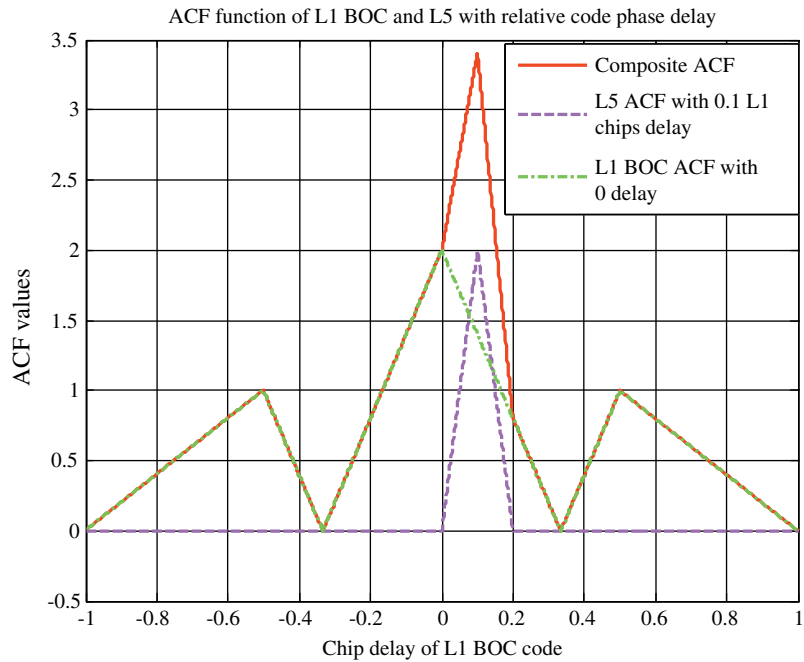


Figure 6. Composite ACF function (red) including worst case relative code delay for E5b (magenta).

losses were found using Equations 5 and 6 given for the GPS case, where for Galileo and assuming DSB processing Equation 5a is used to calculate the correlator spacing loss for L1B, C.

$$CSL_{L1} = 20 \cdot \log \left(1 - \text{abs} \left(|CD_{L5}| - \frac{d_{L5}}{2} \right) \cdot \frac{R_{C,L1}}{R_{C,L5}} \right) \tag{5}$$

$$CSL_{L1} = 20 \cdot \log \left(1 - \text{abs} \left(|CD_{L5}| - \frac{d_{L5}}{2} \right) \cdot \frac{3R_{C,L1}}{R_{C,L5}} \right) \tag{5a}$$

$$CSL_{L5} = 20 \cdot \log \left(1 - \frac{d_{L5}}{2} \right) \tag{6}$$

where CD_{L5} is the relative chip delay in L5 chips.

3.2.3. *Relative carrier phase.* The average carrier phase offset in an integration period will, in general, be different for two signals with different Doppler frequencies. Equation 7 shows this effect at the correlation totals on the *I* and *Q* arms for processing a single signal:

$$\begin{aligned} I_C &= \frac{A}{\sqrt{2}} \cdot \frac{\sin(\pi \cdot \Delta f_1 \cdot T)}{(\pi \cdot \Delta f_1 \cdot T)} \cdot R(\tau) \cdot D_1 \cdot \cos(\Delta \Phi_1) \\ &+ \frac{A}{\sqrt{2}} \cdot \frac{\sin(\pi \cdot \Delta f_2 \cdot T)}{(\pi \cdot \Delta f_2 \cdot T)} \cdot R(\tau) \cdot D_2 \cdot \cos(\Delta \Phi_2) \\ Q_C &= \frac{A}{\sqrt{2}} \cdot \frac{\sin(\pi \cdot \Delta f_1 \cdot T)}{(\pi \cdot \Delta f_1 \cdot T)} \cdot R(\tau) \cdot D_1 \cdot \sin(\Delta \Phi_1) \\ &+ \frac{A}{\sqrt{2}} \cdot \frac{\sin(\pi \cdot \Delta f_2 \cdot T)}{(\pi \cdot \Delta f_2 \cdot T)} \cdot R(\tau) \cdot D_2 \cdot \sin(\Delta \Phi_2) \end{aligned} \tag{7}$$

where A is the signal’s amplitude, Δf_1 is the Doppler error of L1 in Hz, Δf_2 is the Doppler error of L5 (E5b) in Hz, $R(\tau)$ is the cross-correlation function for a delay τ , $\Delta \Phi_1$ is the carrier phase error of L1 and $\Delta \Phi_2$ is the carrier phase error for L5 (E5b). D_1, D_2 are the sign of the data bits, including secondary code and T is the coherent integration period. The carrier phase error in equation 7 can result in a decreased or even total cancellation of the combined signal energy from the two signals. Thus it is crucial to determine combinations of the *I* and *Q* correlation total outputs that would capture the combined signal energy of the two signals. Assisted GNSS architectures would not be able to provide information about the relative carrier phase of the two different frequency signals, which makes the relative carrier phase an additional search space when considering the coherent combination of frequency diverse signals. Equation 8 and Figure 7 depict the situation when the correlation totals of two signals of different frequencies are combined coherently to form the test statistic using the composite *I* and *Q* values.

The combination of *I* and *Q* correlators for the two signals at 90-degree rotations will guarantee a maximum phase-related loss corresponding to a phase offset of 45 degrees, with a worst case energy loss of 0.68 dB. Equation 8 shows the combinations

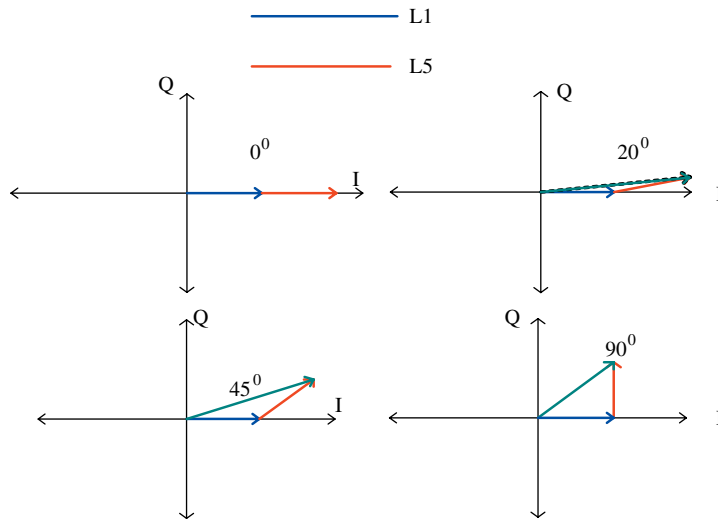


Figure 7. Carrier phase relationships of two signals on different Doppler error.

for two sets of complex correlators I_1-Q_1 for the L1 band and I_2-Q_2 for the L5 carrier.

$$\begin{aligned}
 Comb1 &= (I_1 + I_2)^2 + (Q_1 - Q_2)^2, \\
 Comb2 &= (I_1 - I_2)^2 + (Q_1 + Q_2)^2, \\
 Comb3 &= (I_1 + Q_2)^2 + (I_2 + Q_1)^2, \\
 Comb4 &= (I_1 - Q_2)^2 + (I_2 - Q_1)^2
 \end{aligned} \tag{8}$$

Figures 8 and 9 demonstrate the complementary relationship of the first two combinations against relative carrier phase error and Doppler error assuming a 1-ms coherent integration period and equal received powers. For the GPS case, combining the L1 data and L5 data and pilot signals with no information on the data symbols (stand-alone), eight combinations must be considered to include the relative signs of the data and pilot signals, while for the Galileo case 16 combinations were used to include the effect of the different signs on data and pilot for both L1 and E5b. When assisting data is available and the signs of the data bits of the two frequency signals are known, the number of combinations drop to four as is the case of having two signals on different carriers (the relative data and pilot signs are known). In any case, at each time the maximum of the combinations that have been defined is chosen and compared against a threshold value. If the maximum value of the combinations formed exceeds the threshold then signal detection is declared, otherwise no detection is declared.

4. SIMULATION SETUP. All the losses associated with the combination of signals at different frequencies have been included in the simulations to derive the benefit of such a combination in terms of probability of detection under worst-case scenarios, over the usage of a single signal only. Two approaches can be

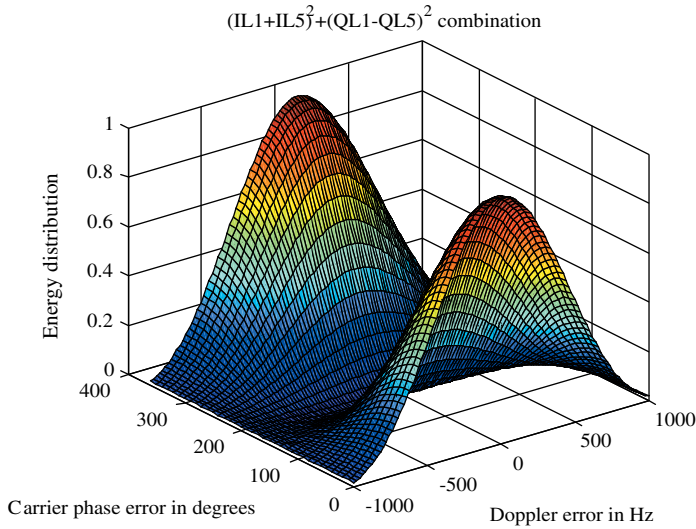


Figure 8. $(I_{L1} + I_{L5})^2 + (Q_{L1} - Q_{L5})^2$ combination.

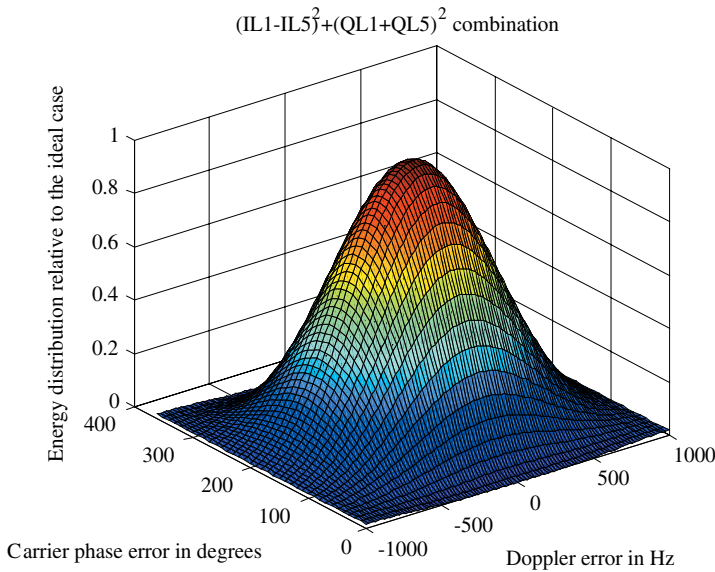


Figure 9. $(I_{L1} - I_{L5})^2 + (Q_{L1} + Q_{L5})^2$ combination.

taken to derive the benefits of the coherent combination of signals. The first is to set the required probability of detection (PD) for each signal combination and compare the resulting probability of false alarm (PFA) for the threshold calculated as a measure of the acquisition time. Alternatively, the probability of false alarm (PFA) can be set adjusting the acquisition threshold for the noise only case and then compare the probability of detection resulting from the different signal combinations.

Assuming the simplest case of single signal acquisition, in the case that there is no signal present in both I and Q , these correlator outputs have a Gaussian distribution. The detection metric is formed as:

$$TST = (I)^2 + (Q)^2 \quad (9)$$

which has a chi-square distribution with two degrees of freedom, since there are two Gaussian distributions that are squared and summed. When signal is present, the detection metric distribution is a non-central chi-square distribution with the same number of degrees of freedom, with the non-centrality parameter depending on the CNR value. The variance of the distribution when there is no signal present is then found by using Equation 10:

$$\sigma_{SC}^2 = 4 \cdot (N \cdot L \cdot V_g)^2 \quad (10)$$

where σ_{SC}^2 is the variance of the chi-square distribution, N is the number of signals that are coherently combined, L is the number of coherent additions that are performed before forming the final detection metric TST , and V_g is the variance of the noise for each of I or Q .

The same case applies when two or more signals are coherently combined, although multiple energy detection metrics resulting from the combinations of the correlation totals are compared to the detection threshold, accumulating to the required PFA value in the noise only case. The number of the detection metrics used depends on the number of combinations that are used to acquire the combined signal energy. This is shown in Equation 11, where the maximum energy detected amongst all the combinations used is compared against the threshold that gives the required PFA value.

$$TST_SC = \max(\text{Combinations}_{1..B}) > \text{Thr}_{PFA} \quad (11)$$

where B is the total number of correlation totals combinations that are used. This method has been referred to in the literature defined as semi-coherent integration [4].

Due to the multiple detection metric comparison that takes place in the case of combining energy from more than one signal, the PFA value is overestimated compared to the case of using a single detection metric as is the case when processing the correlation totals of a single signal. In this work the PD value was set to 0.95 and the threshold was adjusted for all combinations in the case of coherently combining two or more signals, to result in this required probability of detection value, using the resulted PFA value to assess the acquisition performance of the signal combinations used in each case. This method was preferred for the calculation of the performance for each signal combination, rather than calculating the probabilities of detection and false alarms using statistics theory.

Additionally two other signal integration options have been used in the simulations. The first is non-coherent addition of coherent integration periods over longer than the code length:

$$TSTNC1 = \sum_{j=1}^N (I_{jc})^2 + \sum_{j=1}^N (Q_{jc})^2 \quad (12)$$

which has a chi-square distribution with $2 \cdot N$ degrees of freedom where N is the number of signals combined and the subscript c denotes that I and Q values are

the correlation totals of a long coherent integration period. The variance of the noise-only distribution is then given by:

$$\text{NC1_Variance} = 4 \cdot N \cdot (L \cdot V_g)^2 \quad (13)$$

This integration method does not require the use of multiple combinations since the relative carrier phase error or data bit/secondary code sign effect is cancelled in the squared sum of the I and Q correlation totals. The coherent integration period must avoid data bit transitions.

Additionally, non-coherent sums of coherent integration totals can be used for signal detection, referred to as partial coherent processing, expressed as:

$$PC = \sum_{k=1}^W \left[\left(\sum_{j=1}^N I_{jc} \right)^2 + \left(\sum_{j=1}^N Q_{jc} \right)^2 \right] \quad (14)$$

where W denotes the number of the coherent correlation totals that are added non-coherently, assuming that the maximum signal energy is obtained by adding the long coherent integrated I_c of each signal together to form the total energy on I with the same applying to the Q arm. In the latter case the variance of the detection metric is found by using:

$$PC_Variance = 4 \cdot W \cdot (N \cdot L \cdot V_g)^2 \quad (15)$$

where now the number of degrees of freedom are equal to $2 \cdot W$.

The GPS C/A code signal specification, guarantees a minimum EIRP on the Earth's surface of -158.5 dBW [9] although the current power level transmitted by the satellites in the constellation is more than 3 dB higher than that required to achieve the -158.5 dBW level [18]. The L5 EIRP power level is guaranteed to be a minimum of -155 dBW for the total of the I5 and the Q5 signals. Therefore the minimum guaranteed power level for each of the L5 signals is 0.5 dB higher than the power of the L1 C/A signal. This difference in the minimum received power levels has also been incorporated in the simulations to resemble a realistic situation.

For Galileo, the specified minimum received power levels, are at -157 dBW for L1 and -155 dBW for E5, being shared between the data and pilot channels respectively for each frequency. The L1 transmitted power is 2 dB lower than the L5 power, which could limit the advantages offered by the semi-coherent combination of the two frequencies.

5. SIMULATION RESULTS. Simulations were performed for both the GPS and Galileo systems, including all the worst case losses that have been derived considering the issues of combining signals at different frequencies. In these simulations long fully coherent and partial coherent integrations were performed for each of the possible signal combinations, using the information that can be provided by the assisting network. Specifically, a one second fully coherent processing was performed for the cases combining the L1 and L5 signals using the L1 C/A + I5 + Q5, the two data channels L1 C/A + I5 and the data plus pilot on L5 I5 + Q5 for GPS.

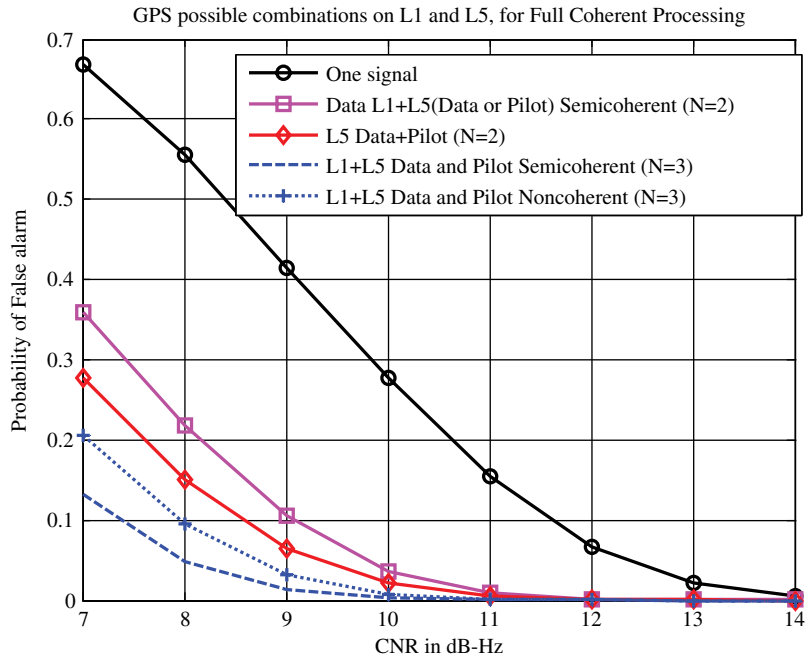


Figure 10. Fully coherent processing of different signal combinations, N is the number of signals used.

The results are shown in Figure 10 where for the single signal case the L5 pilot (Q5) was processed. The magenta line with the square marker shows the PFA values of the combination of two different frequency signals, the L1 data and the L5 data signals, while the red line and the diamond marker represents the PFA values for the combination of the L5 data with L5 pilot signals. As can be seen the L5+Q5 combination results in a better acquisition performance, since there is only one signal combination that is used to compare against a given threshold. In the case of the L1 data with the L5 pilot or data signal though, there are four combinations that have to be tested against a threshold declaring the combination with the maximum value as the correct one, increasing the probability of false alarm.

Another interesting point in Figure 10 is that the non-coherent processing given in Equation 12 using all three available signals, L1 data and the L5 data and pilot shown by the blue dotted line with the cross markers, outperforms both the single and the two signal combinations. The best performance, though, is given by the semi-coherent combination of L1 data with the L5 data and pilot signals given by the blue dashed line.

For Galileo the L1B+L1C+E5bI+E5bQ signal combination case was simulated as well as the combination using the two pilot signals L1C+E5bQ and the E5bI+E5bQ combination. The results of these simulations are shown in Figure 11, where the same conclusions as for the GPS case can be made. Although more signals can be combined with Galileo, the acquisition performance is in general not better than the GPS case, mainly due to the increased losses on the L1B, C signals when using DSB or SSB processing.

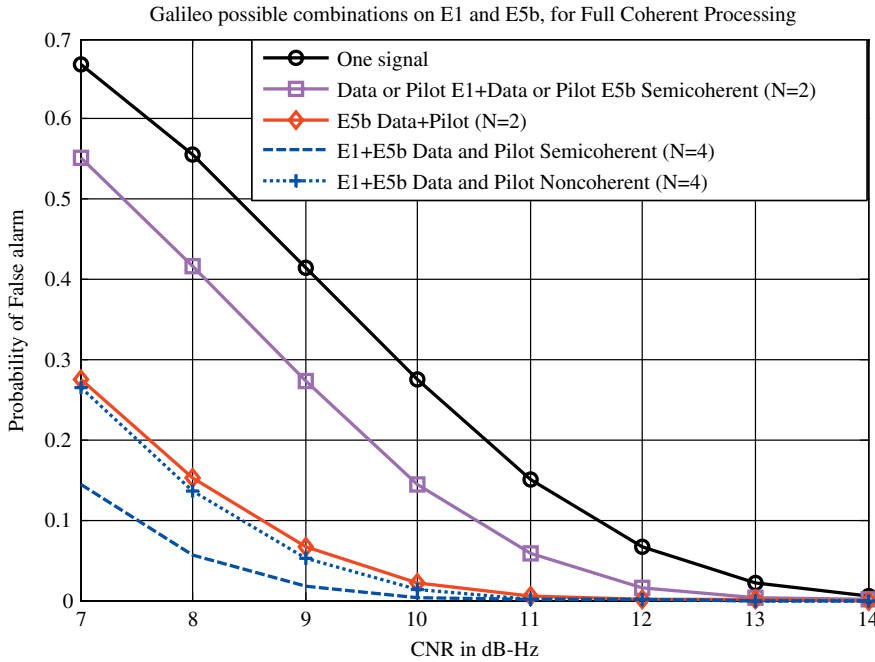


Figure 11. Fully coherent processing of different signal combinations, N is the number of signals.

In addition a 1-sec partial coherent processing was also simulated to evaluate the performance of this processing technique and the potential in the increase of acquisition sensitivity when using coherent combination of signals. Figure 12 shows the results obtained for the GPS case using 50 non-coherent additions of 20-msec consecutive coherent integration periods for the single signal case (L1 C/A) while the setup was changed to 100 non-coherent additions of 10-msec coherent integration periods when the I5 signal was used in the signal combinations, since the coherent integration time is limited by the data bit duration on I5. In this case there is an obvious gain when using longer coherent integration times as was the case for the L1 data signal shown by the black line with the circle markers, using the same correlator spacing as it would apply for the L5 signal. This increases the code search space when using the L1 data signal by 10 times relative to using half of a C/A code chip of correlator spacing, with a clear gain over the sensitivity of the receiver.

6. IMPROVEMENTS TO ACQUISITION TIMES. The results presented in the previous section were concerned with the first energy test taking place in the acquisition process. Detection is assumed when the metric for a combination used to capture the signal energy is greater than the pre-specified threshold. This threshold crossing may also result from a false alarm in the absence of signal through a combination of noise only. After threshold crossing, the acquisition algorithm enters a verification stage, to try to remove any false alarms, which would significantly increase the overall acquisition time. A 2-stage verification algorithm has been chosen in this work to calculate the improvement in terms of

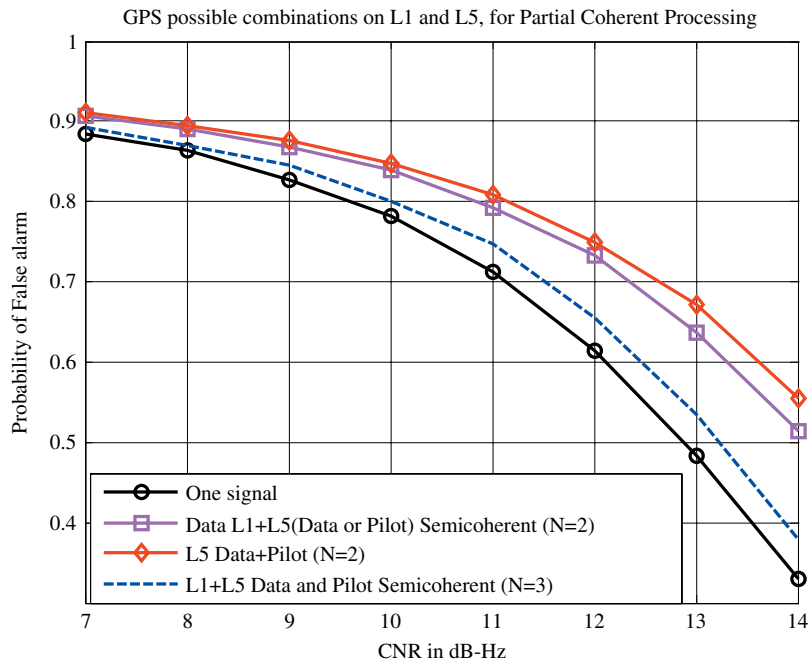


Figure 12. Partial coherent processing of different signal combinations for GPS.

the overall acquisition times, including the verification stages, when using semi-coherent integration of the L1 and L5 signals. The first stage of this verification algorithm is an M out of N search detector [19] followed by a multiple dwell stage. The overall probability of false alarm, or else the probability of entering the tracking stage after the verification algorithm, is the product of the probabilities of false alarms at each individual stage, including the first energy test stage. The same applies for the overall probability of detection.

The multiple dwell stage is to decrease the overall probability of false alarm by using long integration times, while having a low impact on the overall acquisition time, since this long dwell would only be entered after passing the previous verification stages (detection and false alarm phases). In this work we have chosen the 1-sec fully coherent integration results for the GPS case and for the range of CNR values from 7 to 14 dB-Hz to assess the benefit in acquisition time as well.

Figure 13 shows the benefits in the acquisition times using the above described approach, setting the desired overall probability of detection to 0.95 while minimising the overall PFA to a value below 10^{-7} through the verification process, using the data shown in Figure 11. As can be seen at the lowest CNR level the semi-coherent combination of the L1 and L5 GPS signals can result in acquisition times to almost a quarter of the time required when using a single signal. At lower CNRs this improvement seems to be degraded, requiring even longer coherent integration times.

7. CONCLUSIONS AND FUTURE WORK. In this paper, benefits to acquisition from combining signals at different frequencies have been shown,

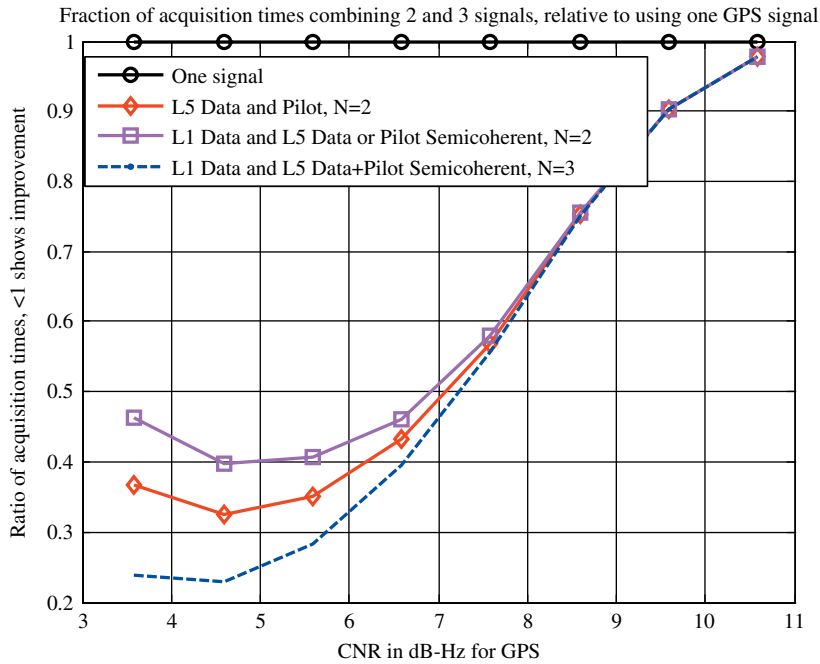


Figure 13. Benefits in acquisition times using semi-coherent combinations of signals for 1-sec of fully coherent integrations times.

mainly focusing on assisted GNSS systems, emphasizing the issues to be considered for such a coherent combination. The proposed method has shown significant benefits in terms of probability of detection during acquisition and in terms of the time that is required to acquire the signal energy, based on the initial acquisition time analysis followed. Further work to improve the acquisition time reductions remains to be done, incorporating optimisation routines that would adjust the coherent integration times, the thresholds that are used in signal detection decisions and the values of M, N for the M out of N search detector as well as the multiple Dwell length, for optimising the acquisition times for each CNR value tested.

Although the benefits were clear for a stand alone GNSS receiver [20], it is shown here that there are benefits when longer coherent integration times than the maximum values in the stand alone case are used as is the case in the assisted GNSS systems. These benefits arise without increasing the search space to match the relative code delay of the signals, which this analysis has showed does not exceed the 100 nanoseconds threshold. Further work [20] has shown that the benefits of the coherent integration of the different frequency signals diminish as the relative code delay exceeds the 500 nanoseconds.

Several architectures that could be used to minimize the relative code delay issue have been considered, while the modelling and the calibration of the relative code delay due to filtering will result in even greater benefits, as the search space will not increase but the alignment of the replica codes with the incoming codes will boost the benefits of the coherent integration of signals at different frequencies.

The benefits that this coherent integration of signal energies at different frequencies can provide to tracking has also to be investigated, identifying the issues that arise in the closed loop operation of a GNSS receiver and finding discriminators that allow the alignment of the phase and frequency of the different signals.

ACKNOWLEDGEMENTS

The work described in this paper has been carried out as part of the SPACE project (Seamless Positioning in All Conditions and Environments), which is an UK Engineering and Physical Sciences Research Council (EPSRC)-funded Pinpoint Faraday flagship project. This project is led by four of the leading academic GNSS research centres in UK and supported by industrial partners. The academic team members are: CAA Institute of Satellite Navigation at University of Leeds, Department of Civil and Environmental Engineering at Imperial College London, Department of Geomatic Engineering at University College London (UCL), and Institute of Engineering Surveying and Space Geodesy at University of Nottingham, and the industrial partners are The Civil Aviation Authority, EADS Astrium, Leica Geosystems, Nottingham Scientific Ltd, Ordnance Survey, QinetiQ and Thales Research and Technology. The primary aim of SPACE is to undertake the basic research needed to build a prototype GNSS-based positioning system that can deliver cm-level accuracy positioning everywhere and at all times.

REFERENCES

- [1] Weill L, (2006) "Theoretical and Practical Sensitivity Limits for Assisted GNSS Receivers Using Legacy and Future GNSS Signals", ION GPS/GNSS 2006
- [2] Van Dierendonck, A. J., (1996) "GPS Receivers" in *Global Positioning System: Theory and Applications*, B. Parkinson and J. J. Spilker, American Institute of Aeronautics and Astronautics, Washington D.C.
- [3] Mattos, P. G., (2003) "Solutions to the Cross-Correlation and Oscillator Stability Problems for Indoor C/A Code GPS", STMicroelectronics, UK, ION GPS/GNSS 2003
- [4] Yang C., Hegarty C. and Tran M., (2004) "Acquisition of the GPS L5 Signal Using Coherent Combining of I5 and Q5", ION GPS/GNSS 2004
- [5] Aguado L. E., Brodin G. J., Cooper J. A. and Alston I. D., (2004) "Combined GPS/Galileo Highly-Configurable High-Accuracy Receiver", ION GPS/GNSS 2004
- [6] Jimenez-Banos D., Blanco-Delgado N., Lopez-Risueno G., Seco-Granados G., Garcia-Rodriguez A., (2006) "Innovative Techniques for GPS Indoor Positioning Using a Snapshot Receiver", ION GNSS 2006.
- [7] Nainesh Agarwal, Julien Basch, Paul Beckmann. (2002) "Algorithms for GPS operation Indoors and Downtown", *GPS Solutions* 2002
- [8] IS-GPS-200 Revision D, 7 March 2006
- [9] ICD-GPS_705, December 2002
- [10] Spilker, Jr., J. J., A. J. Van Dierendonck, (2001) "Proposed New L5 Civil GPS codes", *Journal of the Institute of Navigation*, Fall 2001
- [11] Galileo OS SIS ICD, 23/05/2006
- [12] Hegarty C., Tran M., (2003) "Acquisition Algorithms for the GPS L5 Signal", ION GPS/GNSS 2003
- [13] Wilde W. N., Steewaegen J., Simsky A., Vandewiele C., Peeters E., Grauwen J., Boon F., (2006) "New Fast Signal Acquisition Unit for GPS/Galileo Receivers", *ENC GNSS 2006*.
- [14] Ioannides R. T., Strangeways H. J., (2000), "Ionosphere-induced errors in GPS range-finding using MQP modelling, ray-tracing and Nelder-Mead", *Millenium Conference on Antennas and Propagation*, AP 2000, Davos.
- [15] Erst S. (1984) "Receiving System Design", Artech House.
- [16] Strangeways H. J., Ioannides R. T., (2003) "Determination of errors in finding vertical from slant TEC due to horizontal gradients", *Symposium on Atmospheric Remote Sensing using Satellite Navigation Systems*, Matera, Italy, 13–15 October
- [17] Murata, www.murata.com

- [18] Stevens J. R. A., Brodin G. J., and Cooper J. A., (2004) "Measuring the Effect of Helicopter Rotors on GPS Reception", ION NTM 2004
- [19] Kaplan E., (1996) "Understanding GPS: Principles and Applications", Mobile Communication Series, Artech House.
- [20] Ioannides R. T., Aguado E. A., Brodin G., (2006) "Coherent Integration of Future GNSS signals", ION GNSS 2006